

PACS numbers: 87.50.Y–; 42.79.Jq; 78.20.hb
DOI: 10.1070/QE2012v042n03ABEH014674

In-vitro study of the temperature dependence of the optoacoustic conversion efficiency in biological tissues

S.M. Nikitin, T.D. Khokhlova, I.M. Pelivanov

Abstract. **The applicability of the optoacoustic (OA) method for monitoring temperature during thermal impact on biological tissues is studied experimentally. Tissues under study were chicken breast (as a model of muscle), porcine lard (as a model of fatty tissue) and porcine liver (as a model of richly perfused tissue). The temperature dependences of the amplitude of the OA signals excited in biological tissues were measured *in-vitro* in the temperature range of 20–80 °C under the narrow laser beam conditions. Measurements were performed in two regimes: during heating and cooling. Similarities and differences in the behaviour of the dependences in different temperature ranges associated with different structural composition of the samples were obtained. The accuracy of temperature reconstruction from experimental data for the investigated tissue types was evaluated. It is shown that during tissue coagulation its temperature can be determined with an accuracy of about 1 °C.**

Keywords: *optoacoustic method, high intensity focused ultrasound, optical properties of biological tissues, temperature monitoring, optoacoustic conversion efficiency.*

1. Introduction

Nowadays the problem of developing the methods for local measurement of temperature inside biological tissues is of great importance in medicine. These methods could be used for accurate monitoring of tissue heating during hyperthermia of cancer or during high intensity focused ultrasound therapy (common abbreviation, HIFU). For these purposes, measurements of the temperature distribution should be performed on the time scale less than 1 second (HIFU therapy), providing the spatial resolution of about 1 mm and high temperature sensitivity of about 1 °C [1]. Temperature of an object under study can be measured most accurately using a thermocouple or thermistor. However, this method is invasive because it requires surgical intervention. At the same time, there are some noninvasive methods.

In most methods based on the application of diagnostic ultrasound for temperature monitoring, the temperature dependence of the speed of sound is used [2]. This dependence leads to a shift in the image of the organ subjected to thermal impact. Solving the inverse problem under the approximation of the model of a homogeneous medium, the temperature distribution within the tissue can be reconstructed [3, 4] under the condition that the temperature dependence of the speed of sound for this organ is known. The essential limitation of this method is that not all the tissues can be considered as acoustically homogeneous. In addition, the speed of sound increases with temperature for some tissues, decreases for fatty tissues and even demonstrates first an increase and then a negative slope at temperatures higher than 60 °C for some tissue types [5, 6]. Structural tissue changes caused by coagulation or dehydration also lead to some changes in the speed of sound [7].

IR thermography allows one to perform temperature monitoring in real time with the accuracy of 0.1 °C, but only on the surface of the object [8]. Application of optical methods is also hindered by subsurface tissue layers due to strong light scattering inherent in most tissues [9].

The temperature distribution in the region of the HIFU action can be obtained by the method of the magnetic resonance (MR) thermometry. The typical spatial resolution of the method is 2–6 mm. However, with the temperature sensitivity of ~1 °C the temporal resolution of the method is equal to 1–4 s [10, 11]. This makes it possible to use the MR thermometry only in the case of slow heating [12, 13] when the tissue is damaged within tens of seconds whereas the HIFU therapy, for example, requires milliseconds. Another disadvantage is the high cost and unhandiness of MR systems [10, 11, 14].

Thus, the development of a method that could overcome these limitations, i.e., to be noninvasive, have sufficient spatial resolution, high temperature sensitivity (about 1 °C), high monitoring depth (a few centimetres), and work in real time, is of great practical importance.

To solve the problem of measuring the temperature distribution inside a biological tissue or an organ, an optoacoustic (OA) method can be potentially used [15]. Usually, the nanosecond range of laser pulses is employed to excite OA signals in biological tissues. It allows one to operate in the megahertz range of acoustic frequencies, providing a submillimeter spatial resolution. The amplitude and shape of the excited acoustic signal depends on the optical (light absorption and scattering coefficients) and thermophysical properties of the medium under examination and on the laser fluence within it. These characteristics are temperature dependent; therefore, the amplitude and shape of the excited optoacoustic signal will also depend on the temperature. Because in biological media (media with low thermal conductivity) the speed of ultrasound is usually several orders of magnitude higher than the characteristic speed of heat diffusion, the temperature distribution inside biological tissues can be determined by solving the OA imaging problem [16–18].

S.M. Nikitin, T.D. Khokhlova, I.M. Pelivanov International Laser Center, M.V. Lomonosov Moscow State University, Vorob'evy gory, 119991 Moscow, Russia; e-mail: pelivanov@ilc.edu.ru

Received 15 June 2011; revision received 7 February 2012
Kvantovaya Elektronika **42** (3) 269–276 (2012)
Translated by I.M. Pelivanov

One of the possible applications of the OA method is the monitoring of HIFU therapy of tissues. In HIFU therapy, high-power ultrasound waves are focused inside a human body, which leads to heating due to absorption of ultrasound and to subsequent coagulation necrosis of a tissue region (for example, tumours) in the focal zone of a HIFU transducer [19]. The lesion is then 'dissolved' by the human productive system. This effect is used for the treatment of different tumours [20–22], resulting in their coagulation necrosis, and for stopping blood bleeding [23]. Typically, a single lesion caused by the HIFU action has a length of about 5–10 mm and a cross section of 2–3 mm. For the treatment of a large volume of a tissue, the focal zone of the transducer can be scanned. HIFU therapy has been already used *in vivo* for noninvasive removal of tumours in the breast, prostate, liver, kidney and other organs (see, for example, [19–21]), but the main obstacle to widespread application of this technology in clinics is the lack of reliable methods for monitoring the HIFU procedure, i.e., targeting of the HIFU transducer, imaging of the lesions and online temperature monitoring.

The potential applicability of the OA method in diagnostics of thermal impact induced by HIFU on biological tissues was apparently first demonstrated in [24]. A lesion of sufficiently large size (25 × 3 mm), located at a relatively small depth (~1 cm) inside the tissue (porcine liver), was examined. Due to changes in the optical and thermophysical parameters of the lesion in comparison with that for the surrounding tissue region, the temporal profile of the OA signal had a feature (local maximum). This feature made it possible to determine the location of the lesion that was exposed to focused ultrasound. However, the authors of [24] did not consider the dynamics of the temperature impact (only the contrast between the lesion and the surrounding tissue was observed), i.e., features of OA conversion as functions of tissue heating were not studied.

The sensitivity of the OA signal amplitude to temperature variations within biological tissues was demonstrated in [25]. The temperature dependences of the OA signal amplitude were obtained for canine liver and canine muscle tissue. However, the experiments were performed in the case of a wide probe laser beam. Therefore, the influences of light scattering, light absorption, local laser fluence distribution and Grunaisen parameter on the temperature dependent amplitude of OA signals excited at tissue surface could not be separated. On the other hand, when OA conversion occurs within a small region of a turbid medium, the OA signal amplitude is proportional to the light absorption coefficient of this region and depends very little on light scattering [26]. Thus, the dependences of OA signal amplitude on optical properties of the tissue are different when OA conversion occurs at the tissue surface and inside the tissue. This fact should be taken into account in OA temperature monitoring during HIFU when tissue properties are modified inside a small volume of the tissue.

The temperature dependence of the OA signal amplitude was also studied experimentally in [27]. Turkey muscle tissue was used as a model medium. The tissue sample was placed in a tank of oil with a temperature exceeding the room temperature. Measurements were performed at temperatures varying from the room temperature to the equilibrium one for both media. A disadvantage of [27] was the fact that the temperature field inside the sample was heterogeneous, i.e., the tissue temperature could be different in the surface region, where light was mainly absorbed, and inside, where a thermocouple was placed.

For application of the OA method in medical practice for tissue temperature monitoring during HIFU, it is also necessary to determine the temperature dependence of the OA conversion efficiency for different tissue types, i.e., to get some gauge dependences.

An interesting approach to obtain such gauge dependences was proposed in [28]. The authors inserted nanoparticles within a tissue structure to increase the OA conversion efficiency. They assumed that nanoparticles changed only light absorption of the tissue under study but did not change the OA conversion efficiency (Grunaisen parameter), i.e., the OA signal produced by the particles themselves was ignored. As was shown in [29], this assumption is quite approximate. Furthermore, optical absorption of tissues [12, 22, 23] can be changed if temperature exceeds the coagulation point.

As far as we know, *in-vivo* study of the OA contrast between a HIFU-treated lesion and surrounding healthy tissue was reported only in [30]. The authors were surprised that the OA contrast in a richly perfused tissue (mouse kidney) was negative after the HIFU action. The reason of this fact is still unclear. Despite the growth of the light absorption coefficient due to formation of methemoglobin at high temperatures, coagulation process in a tissue can block the blood circulation and initiate tissue dehydration. These processes can decrease the resulting OA contrast between the lesion and the healthy tissue. We speculate that the resulting contrast can strongly depend on the HIFU regime.

Thus, the problem of OA temperature monitoring looks very complicated and hence requires a stage-by-stage approach. Works performed and briefly described above, do not provide us with the clear recommendation to develop a working prototype of a real-time OA thermometer during the HIFU action.

The aim of this paper was to complement previous works in this area by studying OA conversion in different tissues at different heating/cooling regimes in a wide range of temperatures.

2. OA method

The amplitude of the OA signal excited in an elementary volume of the medium is proportional to the product of the light absorption coefficient μ_a and the OA conversion efficiency $\Gamma = c_0^2\beta/(2c_p)$ (the Gruneisen parameter; c_0 is the speed of sound; β is the coefficient of thermal expansion; and c_p is the specific heat at constant pressure) [15], which depend on temperature. Reconstruction of the temperature distribution inside the tissue can be done by detecting the OA signals, induced by absorption of pulsed laser radiation within a tissue, with a transducer array and finally by solving the inverse problem of OA tomography [15–17], if the gauge dependence of $\mu_a\Gamma$ on temperature for the tissue under study is known.

To measure the gauge dependences, the following method is employed. Let a nanosecond laser pulse fall onto the interface between a transparent medium and the tissue under study. Then, the amplitude of the OA signal excited in the tissues can be expressed as [26]:

$$P_{max} = k\Gamma\mu_a E_0, \tag{1}$$

where $k \equiv E_{max}/E_0$ is the coefficient of an increase in the laser fluence in the surface layer of a turbid medium; E_{max} is the maximal laser fluence in the tissue.

If a medium is homogeneously absorbing and nonscattering, the maximal laser fluence E_{max} is located on the medium surface and equal to the laser fluence E_0 in the incident beam. However, in the case of turbid media the laser fluence E_{max} in the surface layer of the medium may exceed E_0 by 4–6 times due to backscattering. This effect was studied theoretically and experimentally in some papers (see, for example, [31–33]). In this case, the coefficient k depends on the diameter of the laser beam and optical coefficients (absorption and reduced scattering coefficients) [26]. Therefore, the amplitude of the excited OA signal will be determined already by three temperature dependent factors: E_{max}, μ_a, and Γ [see formula (1)]. The change in the parameters E_{max} and μ_a is caused by irreversible changes in the biological tissue, for example, during its coagulation [24, 34, 35] or by formation of methemoglobin in the tissue blood at high temperatures [36, 37], which greatly complicates possible interpretation of the data obtained.

However, in the case of a narrow laser beam, $d \leqslant l^*$ ($l^* = 1/\mu_s'$ is the photon transport mean free path in the medium), which for most tissues in the visible and near-IR range is fulfilled when $d \lesssim 0.5$ mm, the quantity $k(\mu_a/\mu_s')$ is a constant at $0.01 < \mu_a/\mu_s' < 0.3$ [26]. Thus, the diameter of the probe beam can be chosen so that in the subsurface layer of the medium the volume density $\mu_a E_{max}$ of the absorbed laser radiation have similar values at different scattering coefficient and be linearly dependent on the light absorption coefficient μ_a.

Therefore, in the backward detection regime [26], under the conditions of the narrow laser beam and the finite duration of the laser pulse, the OA signal amplitude is proportional to the light absorption coefficient μ_a and depends very little on the reduced light scattering coefficient μ_s'. Then, the temperature dependence of the OA signal amplitude resembles the temperature dependence of the parameter $\mu_a\Gamma$ [the dependence of E_{max} on the temperature, which is related with variations of the light scattering coefficient in the biological tissue, can be eliminated from expression (1)].

Thus, by measuring the temperature dependence of the OA signal amplitude under these conditions for different biological tissues, we can obtain the gauge dependences for the product $\mu_a\Gamma$.

3. Experimental procedure

Radiation of the fundamental harmonic of a Q-switched Nd:YAG laser (1064 nm) with a pulse duration of 12 ns and a pulse repetition rate of 50 Hz was used for the excitation of the OA signals (Fig. 1). The pulse energy could be decreased by a set of neutral light filters and was equal to 2–3 mJ on the surface of a tissue. The laser beam diameter on the surface of a tissue was equal to 2.5 mm. It is important to note that the incident laser fluence, according to [38], was significantly less than the medical safety standards. The tissue samples were heated by less than 0.01 °C by one laser pulse and by less than 1 °C during the entire cycle of measurements when averaging over 128 realisations.

A special beamsplitter was used to deflect laser radiation by 90°. The beamsplitter was made of two (in optical contact) quartz prisms of the triangular cross section. A thin metal layer was deposited on one of the contacting surfaces. This layer was 'acoustically thin', i.e., the OA signal excited in the medium passed through it without considerable reflection losses. The bottom of the beamsplitter was in contact with the tissue under study; from above, through the 7-mm-thick duralumin diaphragm filled with deionised water, – with a

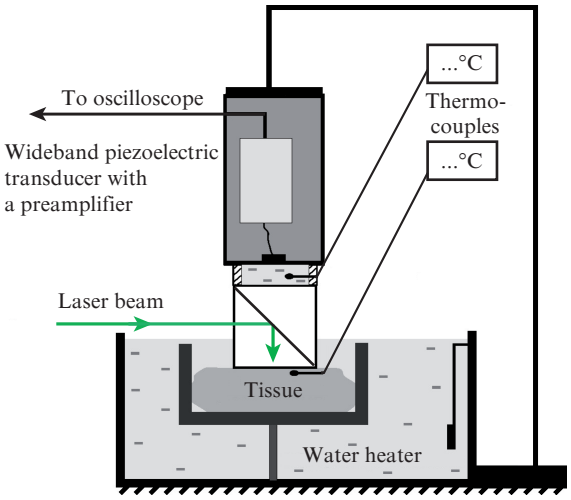

Figure 1. Scheme of the experimental setup.

wideband piezoelectric transducer. The presence of the duralumin diaphragm with water provided nearly constant temperature of the detector during the experiment (the maximum temperature of deionised water near the receiver was additionally monitored with a thermocouple and did not exceed 40 °C). The massive metal housing of the transducer ensured dissipation of heat from its surface. All this made it possible to neglect the pyroelectric effects in the piezoelectric transducer and any change in its temperature sensitivity.

The detector was made of a 110-μm-thick PVDF film. It had a smooth transient response in the frequency range of 0.05–12 MHz, the low-frequency sensitivity was 845 μV Pa^{-1} (with 50-fold amplification). The detected signal was then digitised with the digital Tektronix TDS-1012 oscilloscope (sampling rate, 1 GHz; analogue frequency, 100 MHz). Synchronisation of the system was performed using a photodiode located behind a rear mirror of the laser resonator.

As noted above, the gauge dependencess $\mu_a\Gamma$ are necessary for application of the OA method to monitor temperature in tissues under thermal impact. These calibration curves can be different for tissues with different structural components, i.e., depend on the content of fat, water, muscle tissue and blood. Therefore, as a model media we used porcine liver (the tissue which simulates the properties of richly perfused human tissues), chicken breast (simulating a muscle) and porcine lard (simulating a fatty tissue).

The investigated biological objects were stored no longer than 36 hours after removal from the animal and did not undergo serious temperature impacts (freezing, high-temperature heating). For the experiments we cut samples 3 × 3 × 2 cm in size. They were then placed for a while (~1 h) in a vessel with deionised water under the reduced pressure (~0.5 atm), which made it possible to remove from the tissue air bubbles distorting the temporal profile of excited OA signals.

Following the degassing procedure, the samples were mounted in a holder which was then placed into a heating water bath filled with deionised water. The temperature dependences of the OA signal amplitude were measured in two regimes: heating and cooling of tissues. During heating the temperature of samples was changed from the room temperature (~23 °C) to ~80 °C and during cooling – from ~80 °C to the room temperature. The samples were heated

quite slowly (the temperature was increased by 2 °C for 5 – 10 min) to provide near-homogeneous temperature distribution within the tissue samples. The temperature inside the tissue was additionally monitored with a thermocouple. To perform measurements in the cooling regime, water in the thermostat was mixed with cold water. After reaching the temperature equilibrium between the thermostat and the sample, the measurement of the OA signal amplitude proceeded. For further cooling the procedure was repeated.

To study the relaxation of the $\mu_a\Gamma$ value, the temperature dependence of the OA signal amplitude in the cooling regime was measured starting with temperatures below 78 °C. For this purpose, the sample was heated (with simultaneous measurement of the OA signal amplitude) to a temperature below 78 °C, whereupon the cooling procedure started. Once the sample temperature reached room temperature, the measurement of the OA signal amplitude proceeded again during the heating regime.

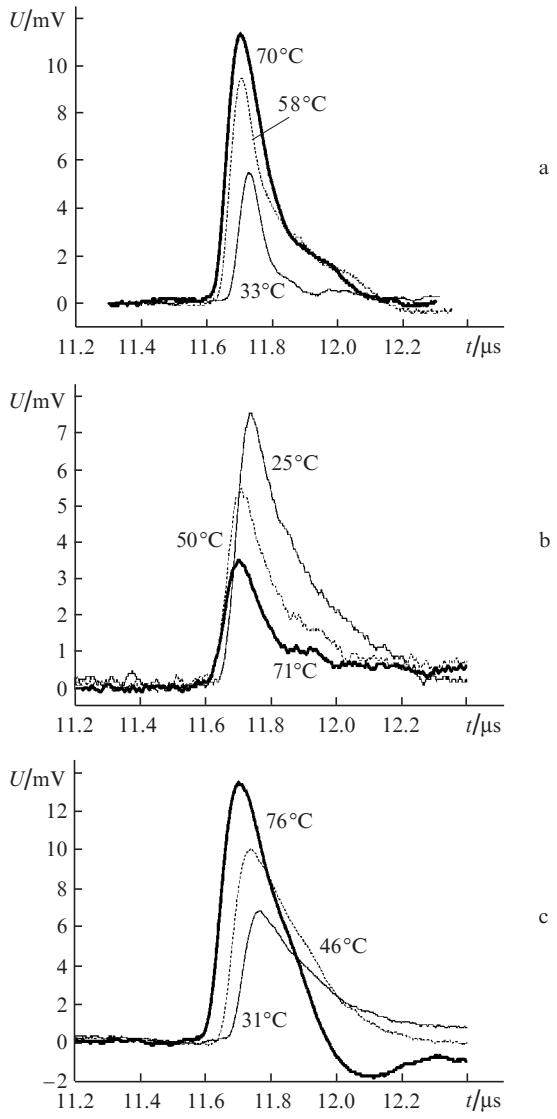

Figure 2. Temporal profiles of OA signals excited in (a) chicken muscle tissue (breast), (b) porcine fatty tissue, and (c) porcine liver samples at different temperatures and detected in the far-field zone by the wideband piezoelectric transducer.

All in all, we studied about 10 samples of each tissue type. The experimental results for three samples of each tissue type are described below. Abbreviations 'A', 'B' and 'C' correspond to all the samples of chicken muscle (breast), porcine fatty tissue and porcine liver, respectively.

4. Results

Typical temporal profiles of the detected signals are shown in Fig. 2. The instant of the OA signal arrival to the detector from the sample surface was approximately 11.7 μs. This time was made up of the time of the OA signal propagation through the beamsplitter (~7 μs) and the diaphragm filled with water (~4.7 μs). Difference in the arrival time of OA signals is explained by the temperature dependence of the speed of sound in the beamsplitter and the water layer being in the contact with the transducer. However, this time shift does not influence the amplitude of detected signals. The temporal profiles show that the OA conversion efficiency in the tissues under study changes. It is interesting that more than a two-fold growth in the OA signal amplitude is observed for the chicken muscle and porcine liver samples when temperature is changed from its room value to 80 °C. At the same time, more than a two-fold decrease in the signal amplitude is observed for the porcine fatty tissue. These dependences are discussed in detail below.

4.1. Chicken muscle

For chicken breast samples, the temperature dependences of the OA signal amplitude are shown in Fig. 3. The OA signal amplitude increased (Fig. 3) with increasing temperature from 25 °C to 70 °C. In some cases (as, for example, for the samples A2, A3) the slope of the dependences became sharper when temperature reached ~45 °C. The OA signal amplitude no longer changed at the temperatures above 70 °C.

When cooling the samples with the initial temperature $T \lesssim 45$ °C, the character of the dependence repeated the heating curve in the inverse direction (Fig. 3, sample A3), i.e., irreversible changes in tissue structure were not observed. When the chicken breast samples with $T > 45$ °C were subjected to cooling, the OA signal amplitude did not return to the initial

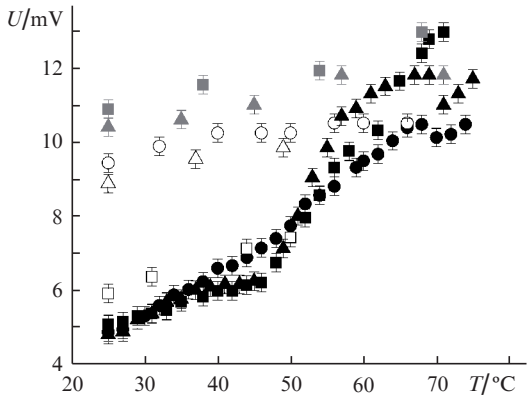

Figure 3. Temperature dependences of the OA signal amplitude for three chicken breast samples during the heating of samples A1 (●), A2 (■) and A3 (▲) from 25 to 78 °C and during the cooling of sample A1 from 66 to 25 °C (○), sample A2 from 50 to 25 °C (□) and from 68 to 25 °C (■), sample A3 from 55 to 25 °C (△) and from 72 to 25 °C (▲).

value thereby revealing irreversible changes in the tissue structure.

4.2. Porcine fatty tissue

The temperature dependences of the OA signal amplitude for different samples of porcine lard are shown in Fig. 4. The main difference in the temperature dependences obtained for the porcine lard from that for the other investigated tissues is that the OA signal amplitude decreases with increasing temperature from 25 to 80 °C. When cooling the samples with the temperature $T \gtrsim 36$ °C (open symbols), the slope of the dependences becomes smoother than that during heating. This may indicate that a partial degradation of the fatty tissue, for example, due to its lipolysis [39, 40], apparently occurs at any temperature exceeding the temperature of a living organism.

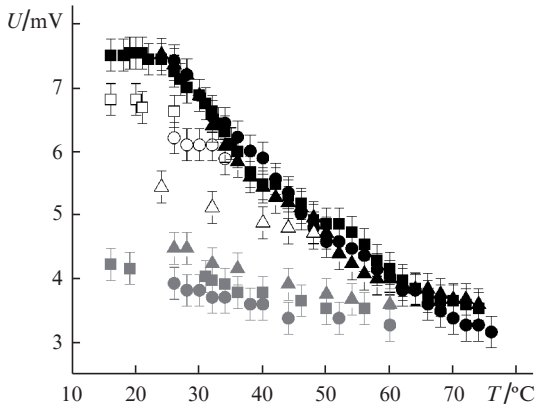

Figure 4. Temperature dependences of the OA signal amplitude for three porcine fatty tissue samples during the heating of samples B1 (●), B2 (■) and B3 (▲) from ~20 to 75 °C and during the cooling of sample B1 from 36 to 26 °C (○) and from 76 to 25 °C (●), sample B2 from 32 to 15 °C (□) and from 65 to 15 °C (■), sample B3 from 50 to 24 °C (△) and from 66 to 25 °C (▲).

4.3. Porcine liver

A characteristic feature of the liver is that that tissue is richly perfused. Blood is the main absorber of optical radiation in the visible and near-IR range. Because the OA signal amplitude is determined by the product $\mu_a\Gamma$, its temperature dependence should experience an additional growth and the behaviour of the OA signal amplitude at high temperatures should be determined by changes in the structure of haemoglobin.

The temperature dependences of the OA signal amplitude for different samples of porcine liver are shown in Fig. 5. Similar to the muscle tissue, when cooling the porcine liver samples with temperatures $T < 45$ °C, the dependence repeated the heating curve in the inverse direction. However, when cooling the samples with $T > 45$ °C, the temperature dependence of OA signal amplitude was linear but with the slope smoother than that during the heating. The OA signal amplitude measured in the initial state of the sample at room temperature differed by more than two times from the OA signal amplitude obtained after the sample was cooled from $T \sim 80$ °C to room temperature. This result agrees well with the results of our previous work [24] when we measured the optical properties of raw and boiled porcine liver tissues. Figure 5

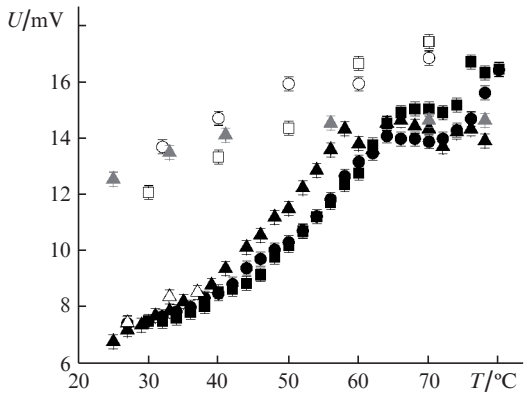

Figure 5. Temperature dependences of the OA signal amplitude for three porcine liver samples during the heating of samples C1 (●), C2 (■) and C3 (▲) from ~25 to ~80 °C and during the cooling of sample C1 from 70 to 30 °C (○), sample C2 from 70 to 30 °C (□), sample C3 from 38 to 27 °C (△) and from 78 to 25 °C (▲).

demonstrates that for most porcine liver samples (samples C1, C2), the OA signal amplitude increased additionally at temperatures above ~72 °C. However, for one of the samples (sample C3) such an additional growth was not observed.

5. Accuracy of temperature reconstruction in tissue

Using the temperature dependences of the OA signal amplitude for different tissues, we can assess accuracy of temperature reconstruction by the OA signal amplitude. To this end, for each type of the tissues the experimental data were divided into several groups corresponding to different temperature ranges. In each of the selected temperature ranges the data were fitted by a straight line with the least-squares method. For example, the temperature dependences of the OA signal amplitude for porcine liver and chicken breast samples changing the slope near 45 °C were divided into two sections: from ~20 to ~45 °C and from ~45 to ~65 °C. The temperature dependences of the OA signal amplitude for porcine fatty tissue samples were fitted with the linear function within the entire temperature range and not divided into sections, because the experimental curves for this tissue did not change the slope significantly. For all the tissue samples the temperature dependences of the OA signal amplitude corresponding to the cooling regime were fitted with one linear function.

The slope and standard deviation for the OA signal amplitude were calculated for all the temperature dependences. After it, the error of the temperature reconstruction was determined. The results of estimating the accuracy of temperature reconstruction from experimental data are presented in Tables 1–3.

6. Discussion and conclusions

As mentioned above, it is important to control the temperature of a tissue during HIFU therapy. The amplitude of the OA signal is proportional to $\mu_a\Gamma$. This coefficient is a function of temperature and thus determines the temperature dependence of the OA signal amplitude.

For the first heating phase of the muscle tissue (chicken breast) (from 23 to ~45 °C; Fig. 3, Table 1) the growth in the

Table 1. Accuracy of temperature reconstruction by the experimental temperature dependence of OA signal amplitude for chicken breast samples.

Sample	Temperature range/°C	Slope/mV °C^{-1}	Standard deviation of OA signal amplitude/mV	Inaccuracy of temperature temperature reconstruction/°C
A1	25–40	0.13	0.08	0.6
	40–65	0.18	0.11	0.6
	66–25	0.028	0.17	6
A2	25–45	0.061	0.05	0.8
	45–65	0.3	0.21	0.7
	55–25	0.063	0.06	1
	72–25	0.048	0.23	4.8
A3	25–45	0.077	0.14	1.8
	50–63	0.32	0.42	1.3
	35–25	0.1	0.1	1
	50–25	0.04	0.15	3.8
	72–25	0.035	0.22	6.3

Table 2. Accuracy of temperature reconstruction by the temperature experimental dependence of OA signal amplitude for porcine liver samples.

Sample	Temperature range/°C	Slope/mV °C^{-1}	Standard deviation of OA signal amplitude/mV	Inaccuracy of temperature temperature reconstruction/°C
B1	20–76	0.063	0.16	2.5
	36–26	0.024	0.05	2.1
	76–25	0.014	0.045	3.2
B2	25–75	0.1	0.26	2.6
	32–15	0.026	0.07	2.7
	65–15	0.024	0.065	2.7
B3	25–75	0.08	0.33	4.1
	30–25	0.04	0.06	1.5
	50–24	0.03	0.046	1.5
	66–25	0.027	0.056	2.1

Table 3. Accuracy of temperature reconstruction by the experimental temperature dependence of OA signal amplitude for porcine lard samples.

Sample	Temperature range/°C	Slope/mV °C^{-1}	Standard deviation of OA signal amplitude/mV	Inaccuracy of temperature temperature reconstruction/°C
C1	27–42	0.093	0.11	1.2
	44–64	0.04	0.22	0.9
	70–30	0.076	0.38	5
C2	30–42	0.08	0.12	1.5
	44–62	0.206	0.12	0.6
	70–30	0.11	0.3	2.7
C3	24–42	0.14	0.1	0.7
	44–58	0.286	0.15	0.5
	38–27	0.107	0.2	1.9
	55–27	0.062	0.15	2.5
	78–25	0.041	0.4	9.7

OA signal amplitude with the temperature is almost linear, which is apparently associated with an increase in the thermal expansion coefficient of water [41] present in that tissue. A more dramatic increase in the OA signal amplitude with increasing temperature (from ~45 to ~70 °C) may be partly associated with an abrupt increase in the scattering coefficient (by more than two times [24]) during the protein tissue coagulation, and consequently in E_{max} (1). Because the laser beam diameter was greater than the photon transport mean free path in the medium, the increase in the light scattering coefficient could lead to an additional growth (~20%) of the OA signal amplitude. However, changes in the heat capacity of a tissue or its thermal expansion coefficient are more likely. When the temperature exceeded ~70 °C (Fig. 3), the signal amplitude remained virtually unchanged, which may be associated with dehydration of the tissue during coagulation of protein components and their partial destruction. If the chicken breast samples with the temperature $T \lesssim 45$ °C were cooled, the amplitude of the OA signal returned back to its original value, which apparently indicates the absence of irreversible changes in protein components contained in the tissue until the coagulation threshold. However, when chicken breast samples were cooled starting with the temperatures exceeding $T > 46$ °C, the slope in the temperature dependences became smoother than that during the heating regime. This indicates that some irreversible structural changes occur

in the biological tissue at temperatures above the coagulation point.

The main difference in temperature dependences measured in fatty tissue samples (Fig. 4) from two other tissues is that the OA signal amplitude decreases with the increasing temperature from 25 to 80 °C. This decrease occurs steadily and without any significant changes in the slope within the entire temperature range under study. However when cooling the samples with $T \gtrsim 36$ °C, the OA signal amplitude does not return to its initial value at room temperature. This is apparently caused by the fact that structural changes in the fatty tissue occur at any temperatures exceeding the temperature of a living organism.

The reason for the examination of the porcine liver is explained by the fact that it is very close in its properties to the human liver and is a very good example of a richly perfused tissue. In addition, porcine liver contains fats, proteins, and blood. As was expected (see Fig. 5), the absolute value of the OA signal amplitude is much larger than that for the chicken muscle due to presence of some volume of blood. However, the temperature dependences of the OA signal amplitude are similar to those obtained for the chicken breast sample, except the region of high temperatures (above ~72 °C), where the OA signal amplitude starts increasing again for most samples. This fact can be explained by the formation of the methemoglobin in blood, which leads to an increase in the light absorption coefficient [32]. Note, however, that for one of the samples (C3), an additional growth of the OA signal amplitude was not observed. This fact can be related to a local (within the laser beam diameter of 2 mm) inhomogeneity of the tissue sample, i.e., with the lack or even absence of blood vasculature in the irradiated region of the tissue. The behaviour of temperature dependences for porcine liver samples in the cooling regime did not differ from that of the dependences obtained for the chicken breast tissue. It can be considered as a justification of the hypothesis that the volume thermal expansion coefficient changes after coagulation of protein components contained in the tissue.

A very important feature of all the types of protein-containing tissues investigated in the this paper is the 'memory' of the temperature dependences for all types of biological tissues containing protein components during their heating above ~45 °C. Indeed, the OA signal amplitude depends not only on the current temperature of the tissue but also on the prehistory of its heating. In case of fatty tissues such a feature reveals already at temperatures exceeding that for a living organism. This fact justifies again the necessity to develop the methods of real-time temperature monitoring in tissues during their heating.

For each of the three tissues under study we estimated the accuracy of temperature reconstruction from experimentally obtained gauge dependences (Tables 1–3). It is shown that the temperature of porcine liver and chicken breast tissues in the region from 25 to ~45 °C can be determined with an accuracy no worse than 2 °C. In the area of tissue coagulation the temperature can be reconstructed with the accuracy of about 1 °C. This is explained by a more rapid growth of the OA signal amplitude in this temperature region.

The experimentally obtained gauge dependences will be used in experiments with a local source of thermal impact, for example, with a HIFU transducer. We hope that obtained results will be useful for the development of OA methods and devices for *in-vivo* temperature monitoring in biological tissues and organs.

Acknowledgements. This work was partially supported by the Russian Foundation for Basic Research (Grant Nos 07-02-00940-a, 10-02-01468-a) and International Science and Technology Center (Project No. 3691).

References

1. Larina I.V., Larin K.V., Esenaliev R.O. *J. Phys. D*, **38**, 2633 (2005).
2. Nasoni R.L., Bowena T., Connora W.G., Sholesa R.R. *Ultrason. Imaging*, **1**, 34 (1979).
3. Farny C.H., Clement G.T. *Ultrasound Med. Biol*., **35**, 1995 (2009).
4. Stepanishen P.R., Benjamin K.C. *J. Acoust. Soc. Am*., **71**, 803 (1982).
5. Bamber J., Hill C. *Ultrasound Med. Biol*., **5**, 149 (1979).
6. Duck F.A. *Physical Properties of Tissue* (London: Academic Press, 1990).
7. Techavipoo U., Varghese T., Chen Q., Stiles T.A., Zagzebski J.A., Frank G.R. *J. Acoust. Soc. Am*., **115**, 2859 (2004).
8. Welch J., Van Gemert M.J.C. *Optical-Thermal Response of Laser-Irradiated Tissue* (New York: Plenum Press, 1995).
9. Tuchin V.V. *Handbook of Optical Biomedical Diagnostics* (Bellingham: SPIE Press, 2007).
10. Köhler M.O., de Senneville D.B., Quesson B., Moonen C.T., Ries M. *Magn. Reson. Med*., **66**, 102 (2011).
11. Furusawa H., Namba K., Thomsen S., Akiyama F., Bendet A., Tanaka C., Yasuda Y., Nakahara H. *J. Am. Coll. Surg.*, **203**, 54 (2006).
12. Hynynen K., McDannold N. *Int. J. Hyperthermia*, **20**, 725 (2004).
13. Larrat B., Pernot M., Aubry J.F., Dervishi E., Sinkus R., Seilhean D., Marie Y., Boch A.L., Fink M., Tanter M. *Phys. Med. Biol*., **55**, 365 (2010).
14. Kuroda K. *Int. J. Hyperthermia*, **21**, 547 (2005).
15. Gusev V.E., Karabutov A.A. *Lazernaya optoakustika* (Laser Optoacoustics) (Moscow: Nauka, 1991).
16. Li H., Wang L.V. *Phys. Med. Biol*., **54**, R59 (2009).
17. Kruger R.A., Kiser W.L., Reinecke D.R., Kruger G.A. *Medical Phys*., **30**, 856 (2003).
18. Khokhlova T.D., Pelivanov I.M., Karabutov A.A. *Akust. Zh*., **55**, 672 (2009).
19. Bailey M.R., Khokhlova V.A., Sapozhnikov O.A., Kargl S.G., Crum L.A. *Akust. Zh*., **49**, 437 (2003).
20. Haar G.T., Coussios C. *Int. J. Hyperthermia*, **23** (2), 89 (2007).
21. Kennedy J.E. *Nat. Rev. Cancer*, **5** (4), 321 (2005).
22. Zhou Y.-F. *World J. Clin. Oncol*., **2** (1), 8 (2011).
23. Hwang J.H., Vaezy S., Martin R., Cho M.-Y., Noble M.L., Crum L.A., Kimmey M. *Gastrointest. Endosc*., **58**, 111 (2003).
24. Khokhlova T.D., Pelivanov I.M., Sapozhnikov O.A., Solomatin V.S., Karabutov A.A. *Kvantovaya Elektron*., **36**, 1097 (2006) [*Quantum Electron*., **36**, 1097 (2006)].
25. Esenaliev R.O., Larina I.V., Larin K.V. *Proc. SPIE Int. Soc. Opt. Eng*., **3594**, 1 (1999).
26. Pelivanov I.M., Barskaya M.I., Podymova N.B., Khokhlova T.D., Karabutov A.A. *Kvantovaya Elektron*., **39**, 830 (2009) [*Quantum Electron*., **39**, 830 (2009)].
27. Pramanik M., Wang L.V. *J. Biomed. Opt*., **14**, 054024 (2009).
28. Shah J., Park S., Aglyamov S., Larson T., Ma L., Sokolov K., Johnston K., Miller T., Emelianov S. *J. Biomed. Opt*., **13**, 034024 (2008).
29. Inkov V.N., Karabutov A.A., Pelivanov I.M. *Laser Phys*., **12**, 1283 (2001).
30. Chitnis P.V., Brecht H.-P., Su R., Oraevsky A.A. *J. Biomed. Opt*., **15**, 021313 (2010).
31. Grashin P.S., Karabutov A.A., Oraevsky A.A., Pelivanov I.M., Podymova N.B., Savateeva E.V., Solomatin V.S. *Kvantovaya Elektron.*, **32**, 868 (2002) [*Quantum Electron*., **32**, 868 (2002)].
32. Tuchin V.V., Utz S.R., Yaroslavsky I.V. *Opt. Eng*., **33**, 3178 (1994).
33. Star W.M. *Phys. Med. Biol*., **42**, 763 (1997).
34. Ritz J.P., Roggan A., Germer C.T., Isbert C., Muller G., Buhr H.J. *Lasers Surg. Med.*, **28**, 307 (2001).
35. Yaroslavsky A.N., Schulze P.C., Yaroslavsky I.V., Schober R., Ulrich F., Schwartz H.J. *Phys. Med. Biol*., **47**, 2059 (2002).

36. Lee J., El-Abaddi N., Duke A., Cerussi A.E., Brenner M., Tromberg B.J. *J. Appl. Physiol.*, **100**, 615 (2006).
37. Black J.F., Barton J.K. *Photochem. Photobiol.*, **80**, 89 (2004).
38. Wang L.V. *Photoacoustic Imaging and Spectroscopy* (New York: CRC Press, 2009).
39. Dubrovskii V.A., Yanina I.Yu., Tuchin V.V. *Biofiz.*, **56**, 425 (2011).
40. Dubrovskii V.A., Dvorkin B.A., Yanina I.Yu., Tuchin V.V. *Tsitologiya*, **53**, 423 (2011).
41. Grigoriev I.S., Meilikhov E.Z. (Eds) *Handbook of Physical Quantities* (Boca Raton, NY, London: CRC Press, 1996; Moscow: Energoatomizdat, 1991).